Journal of Structural Geology, Vol. 11, No. 1/2, pp. 191 to 209, 1989
Printed in Great Britain

0191-8141/89 $03.00 + 0.00

Emplacement kinematics of a granite diapir: the Chindamora batholith, Zimbabwe

JOHN G. RAMSAY

Geologisches Institut, ETH-Zentrum, CH-8092 Zurich, Switzerland

(*Received* 8 *March* 1988; *accepted* 11 *November* 1988)

Abstract—The geometric features of a large (50 × 40 km) granitic batholith and its surrounding greenstone belt envelope are described. The batholith is made up of several intrusive components and an intrusion sequence based on contact relations and xenoliths has been established. The igneous rocks show a local foliation (*S*-fabric) and preferred orientation of minerals. The intensity of this fabric accords with the finite strain determined from xenolith shape analysis. When the strain variations are analysed in detail it appears that the batholith was built up by a succession of magmatic pulses each of which led to a stretching of the previously consolidated igneous material — so called 'balloon' tectonics. Evidence is presented that xenolith deformation commences only when the surrounding igneous material has crystallized, and a method is suggested whereby the position of the surface separating crystal supported phase (plastic behaviour) from melt supported phase (liquid behaviour) at different stages in the plutonic history can be determined. Ductile shear zones are present and their geometry accords well with the shape changes necessary to allow the outer parts of the pluton to stretch.

INTRODUCTION

THIS paper describes the results of a structural reconnaissance of one of the many known large composite dome-like batholiths of granitic and tonalitic rock which make up the Archaean craton of Zimbabwe. McGregor (1951) drew attention to the regional distribution of these batholiths and he showed that their surface outcrops were subelliptical, and that individual batholiths were sometimes separated by keel-shaped synclines filled with basic and acid volcanic material and sediments of the Shamvaian and Bulawayan systems now collectively grouped under the term 'greenstone belt' (Fig. 1). McGregor suggested that this pattern of gregarious batholiths had arisen by the diapiric rise of magmatic material, and that this pattern might be characteristic of Archaean tectonic processes. Talbot (1968) gave a more detailed discussion of the emplacement mechanism and suggested that it could best be attributed to thermal convection aided by the gravitational instability resulting from the presence of granitic material of low density below the denser basic volcanics of the greenstone belts. Several other workers have also regarded the Chindamora batholith as a typical example of a diapiric pluton (Anhaeusser *et al.* 1969, Viljoen & Viljoen 1969, Phaup 1973, Viewing & Harrison 1973), but an alternative view was put forward by Snowden & Bickle (1976). They produced structural evidence which suggested that the domal granite mass resulted from the interference of folds of two separate deformation phases and that the granite was located at the mutual culmination of two crossing antiformal structures. Snowden & Snowden (1979, 1981) now accept that the situation is perhaps more complex, and interpret the form as arising from superposed folding together with multiple intrusion of various plutons.

In view of the fundamental importance of the evolution of these granitic domes in understanding the early history of the Earth's crust it was thought profitable to investigate further the geometric structure of one of these batholiths. The Chindamora batholith (Figs. 1 and 2) was selected because of ease of access and excellence of natural exposure. It had the added advantage that the granite area is almost completely surrounded by a margin of greenstone belt material and it is a simple matter to demarcate the rocks comprising it from those making up adjacent batholiths.

The batholith is centred about 55 km north east of Harare. It has a subelliptical form (50 × 40 km, area about 1200 sq.km) with its long axis trending east–west.

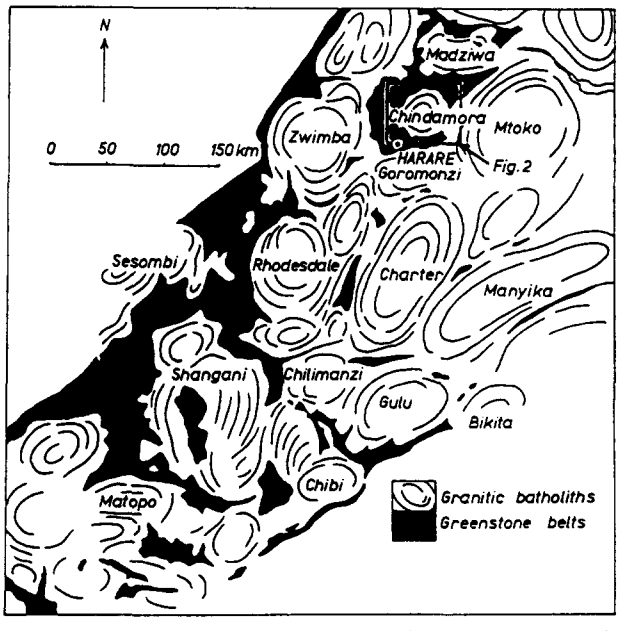

Fig. 1. General map of the Archaean craton of Zimbabwe showing the distribution of granitic batholiths and greenstone belts, after McGregor (1951).

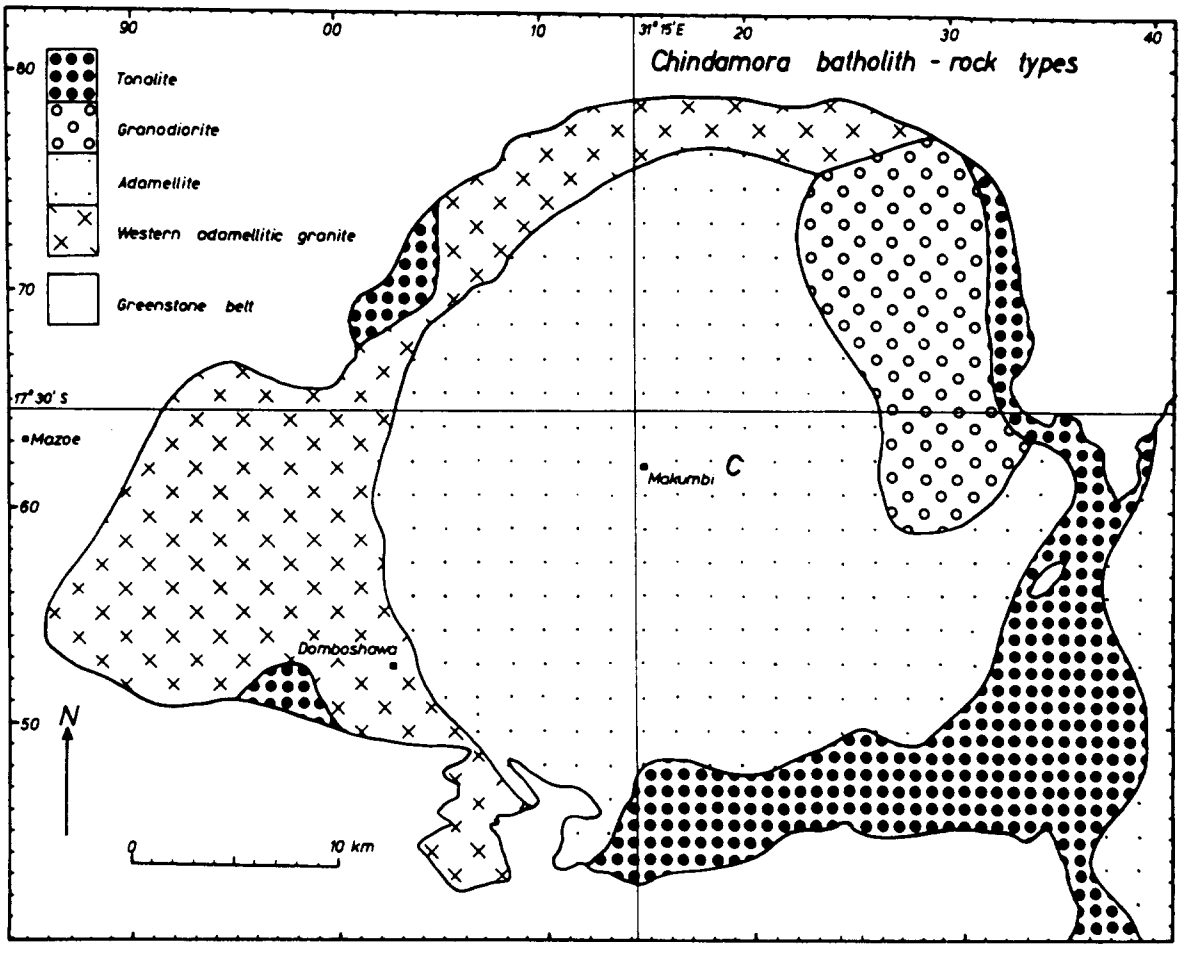

Fig. 2. Geological map of the Chindamora batholith. The intrusion sequence is 1. tonalite, 2. granodiorite, 3. adamellite, 4. western adamellite. C represents the 'centre of gravity' of the central adamellite mass.

The ages of the intrusions making up this batholith are not completely certain but lie between 2750 and 2550 Ma (Snowden & Snowden 1981).

The exposure is generally excellent combining large areas of bare rock pavement with rounded bosses of rock (bornhardts). Although most of the exposure surfaces are subhorizontal it is possible to obtain a three-dimensional view of the structures from occasional steeply inclined surfaces along natural fractures, joints and faults. Exposure in the greenstone belts is generally very poor. Nowhere was the contact between the batholith and its envelope clearly seen. The investigation was carried out by traversing the many good dirt roads. At some 250 selected localities the orientations of structural features were recorded, an integrating scintellometer was used to measure the emission of beta-particles and provided an excellent method of rapidly differentiating different rock types on their radioactive properties. The geological map (Fig. 2) is based on the 1:50,000 maps of the Topographic Survey of Zimbabwe and is of a reconnaissance nature. The original data were collected in 1969 and have been lying unpublished in an office drawer. Hopefully data do not deteriorate with time.

THE ROCK TYPES

The Chindamora batholith is comprised of a number of different types of granitoid rocks (Fig. 2) which show features which can be best attributed to intrusive emplacement of successive magmas (Cloos 1936, Balk 1937). The contrasts between the successive intrusion are all knife sharp and the later magmas contain xenolithic blocks or both greenstone-belt rocks and earlier consolidated igneous rocks (Fig. 3). The xenoliths in the contract area of any particular intrusive component are angular and appear to have shapes controlled by early formed fractures, whereas those some distance from the contact show a more rounded form due to deformation and possibly also to modifications by partial assimilation in the magma. Using the structural relationships observed along contacts and from xenoliths it was possible to establish an intrusion sequence: 1. tonalite, 2. granodiorite, 3. central adamellite, 4. western adamellitic granite. Snowden & Snowden (1979, 1981) have subdivided the igneous suites into a larger number of components, but the overall classification used in this present paper seems to categorize their varieties. The principal mineralogical and structural features of these rocks will now be briefly described.

Tonalite

These are dark, medium-grain size rocks with abundant biotite and amphibole. There is always a strong planar alignment of the crystalline components (Fig. 3) and sometimes a banded gneissic texture. Xenoliths of

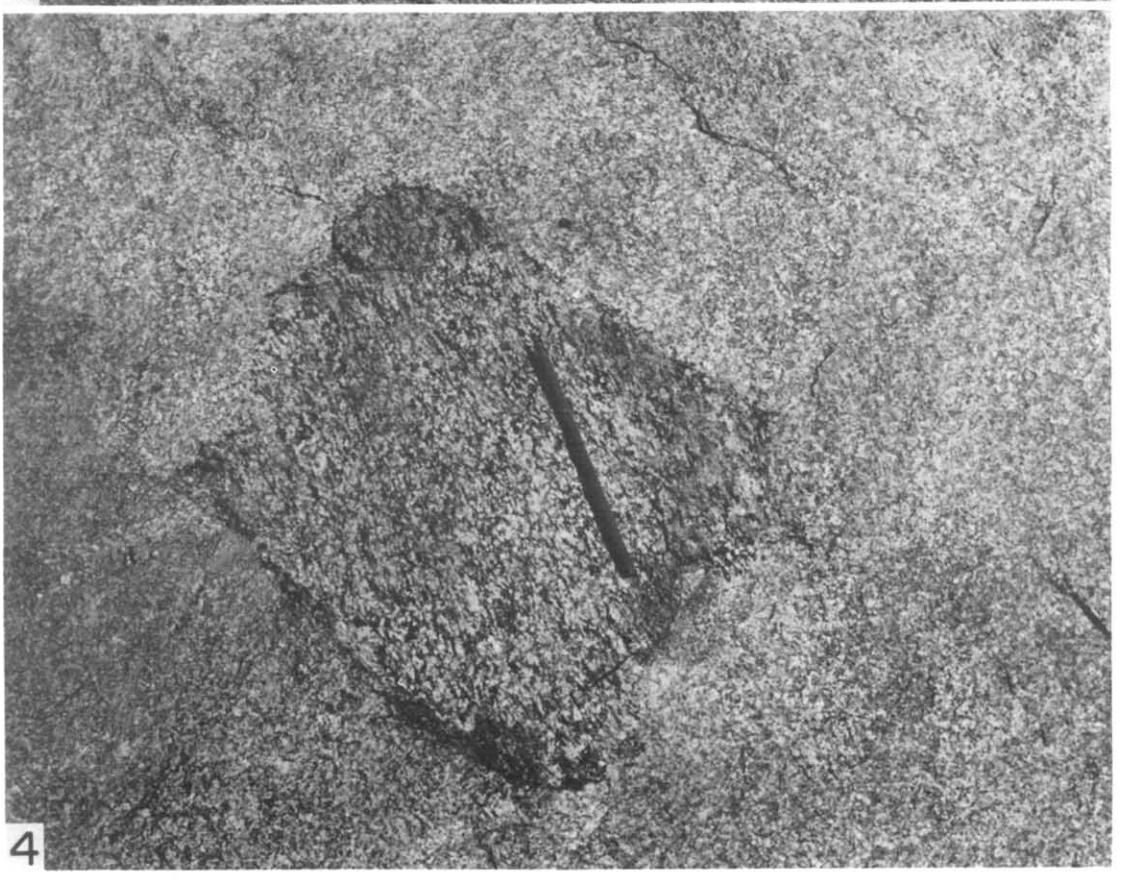

Fig. 3. Cognate xenoliths of tonalite in pale adamellite. The tonalite contains xenoliths of amphibolite (greenstone belt country rocks) and, in contrast to the adamellite, is strongly schistose. Locality 240500. Pencil for scale.

Fig. 4. Strongly schistose subangular xenolithic block of tonalite in adamellite. Locality 154533.

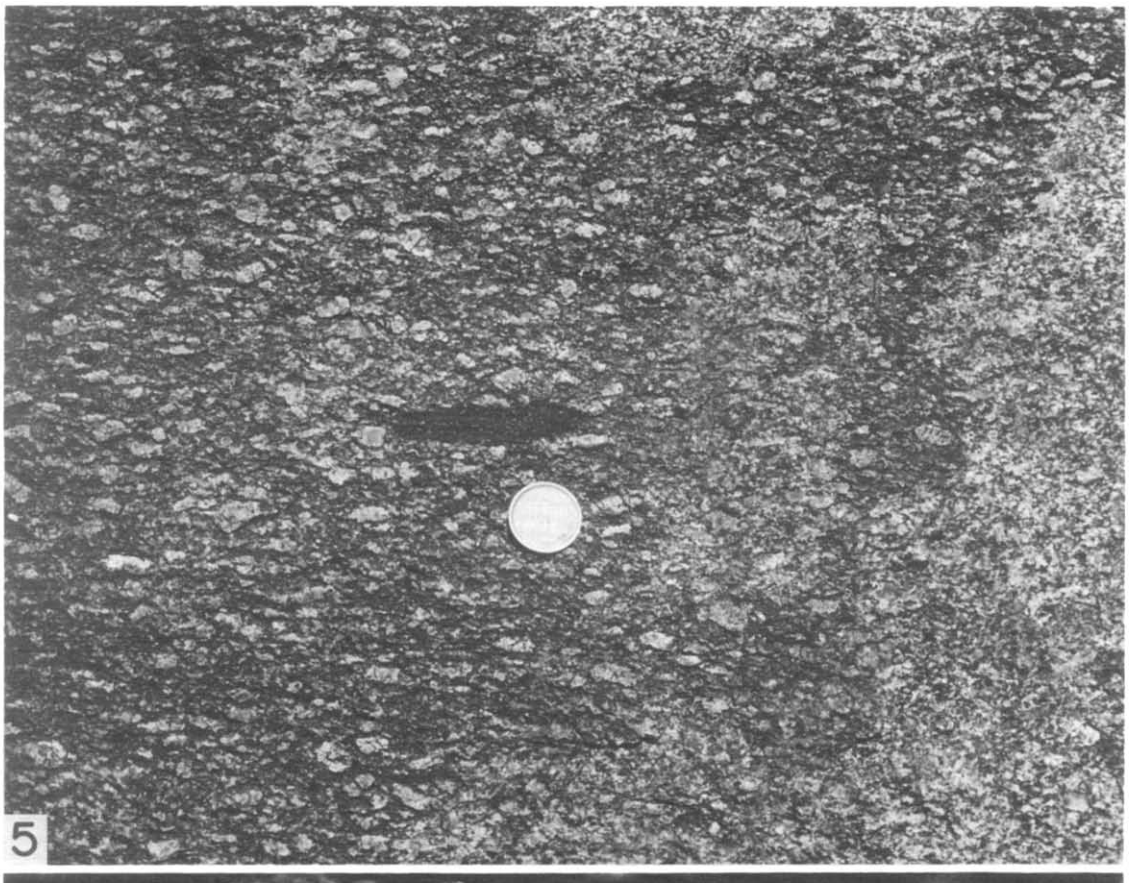

Fig. 5. Adamellite with a pronounced orientation of potassium feldspar crystals showing an elongated (deformed) xenolith of tonalite with the xenolith long axis parallel to the fabric in the adamellite. Locality 223695.

Fig. 6. Strongly deformed ignimbritic rock close to the northwest contact of the batholith. Locality 004696.

Fig. 7. Ductile shear zone cutting tonalite containing acidic dykes. Locality 370597.

rock fragments which match those of the greenstone belts are usually very abundant (Fig. 3). The ratio of potassic felspar to plagioclase is usually less than 1 to 8 and the rocks have a low radioactivity and low beta-particle emission. The largest areas of tonalite are always situated along the margins of the batholith. A few quite large (100 m) masses are found near the centre of the batholith, and these probably represent roof pendants or macro-xenoliths.

Granodiorite

A medium-grained dark grey granodiorite is seen in the north eastern part of the intrusive complex. It shows a strong schistosity produced by a planar preferred orientation of the constituent minerals. Xenoliths of basic volcanic material from the greenstone belt and of tonalite are locally abundant.

Central adamellite

These rocks are very extensive and make up the major part of the centre of the batholith. They are pale grey and commonly the potassic felspars show a reddish-brown colouration. The grain size varies from fine to very coarse. Particularly spectacular are some very coarse porphyritic types with large crystals of inclusion zoned microcline. The adamellite and its associated microgranite, aplite and pegmatite dykes intrude the tonalite and granodiorite, and angular cognate xenoliths of schistose granodiorite or tonalite can be found at some localities (Fig. 4). These cognate xenoliths often show a strong planar fabric (Fig. 4) and contain deformed xenoliths of amphibolite indicating that the tonalite had suffered a deformation before emplacement of the adamellite (Fig. 3). Although most of the adamellite shows little or no schistosity, locally in the outermost part of the intrusion the microcline phenocrysts show a good planar orientation (Fig. 5).

Western adamellitic granite

Along the western and northern border of the batholith a medium- or fine-grained homogenous non-porphyritic adamellitic granite is found. These rocks are chemically and mineralogically similar to the central adamellite, although they have a somewhat lower potassium content. Schistosity is absent or very weakly developed.

Rocks of the greenstone belt

The greenstone belts are made up of acid and basic volcanics (both extrusive and pyroclastic) with extensive developments of acid ignimbrites along the northwest margin of the batholith. Volcanic conglomerates, sandstones, shales and calcareous sediments are also present. The whole assemblage has suffered low grade metamorphism to amphibolite, talc–chlorite–sericite schist, marble and various calc-silicate assemblages of greenschist facies. All these rocks are strongly schistose (Fig. 6); the strike of the schistosity is subparallel to the batholith contact. Practically all rocks found in the greenstone belts tend to be very deeply weathered.

STRUCTURES IN THE BATHOLITH

The granite rocks show a variety of structural features. Some of these features were developed when the material was ductile, whereas others appear to represent late stage geometric modifications when the intrusion was in a near-solid state. The nature and orientation of mineral fabrics, xenoliths, shear zones and fractures were recorded at some 250 localities through the batholith. Many of the geometrical relationship of these structures to the overall batholith form accord quite well with the classic discussions of pluton geometry (Balk 1937), but the interpretation of their significance discussed later is novel.

Foliation

This is a compositional layering produced either by variations in the amounts of the different crystal species or by variations in the crystal size of a single mineral species. It is not a particularly well marked feature and it is most frequent in the external zones of the central adamellites near the contact of this rock with the tonalitic outermost marginal phase. The foliation is probably formed by flow mechanisms, leading to a sorting of the crystals contained in the magma according to size, shape and perhaps density. It appears to form in planes parallel to the walls of the intrusion.

Mineral alignment and schistosity

At many localities mineral species which have a platy or acicular habit show a statistically preferred orientation defining a planar structure (Fig. 5). The penetrative fabric formed in this way is analogous to the tectonically formed fabric known as schistosity. The schistosity in the plutonic rocks is parallel to, and appears to be cogenetic with, the schistosity seen in the deformed volcanic and sedimentary rocks which make up the envelope of the batholith. Biotite and amphibole are the main schistosity forming minerals in the tonalite and granodiorite, and porphyritic microcline and biotite give rise to the fabric in the adamellite. Where schistosity and foliation occur together in the same rock they are very nearly parallel, but at several localities the schistosity clearly cross-cuts the foliation showing that the two types of planar fabric are independent of each other. The intensity of the schistosity varies through the batholith. It is strongest in the outer tonalite and granodiorite, and weakest in the central adamellite and in the western adamellitic granites. The strike of the schistosity is generally subparallel to the contacts of the batholith, and the structure is concentrically disposed around the intrusion centre. The dip of the schistosity at the present erosion level is

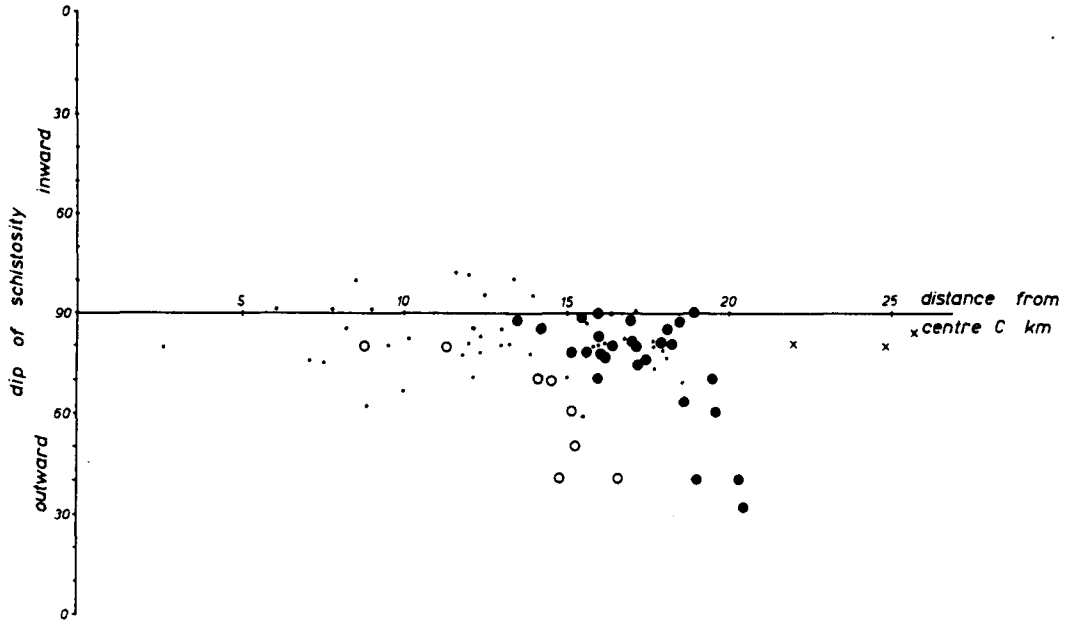

Fig. 8. Variation of dips of schistosity with distance from the batholith centre (C in Fig. 2). Large dots tonalite, open circles granodiorite, small dots central adamellite, crosses western adamellite.

steep in the central part of the batholith; it is sometimes observed to dip towards, sometimes away from, the centre. In the outer parts there is more of a tendency for outward dipping orientations, particularly in the tonalite along the south eastern contact (Fig. 8).

The significance of schistosity is apparent when the finite strains are computed from the shapes of deformed xenoliths (see below). The schistosity is always oriented perpendicular to the direction of maximum finite shortening (i.e. perpendicular to the Z axis of the finite strain ellipsoid with axes $X > Y > Z$) and the intensity of the schistosity increases as the amount of strain increases. At two localities near the edge of the batholith a steeply inclined linear mineral alignment was found on the schistosity surfaces, this lineation being parallel to the X direction of the strain ellipsoid.

Xenoliths

Many of the granitic rocks exposed in the batholith have angular, subangular or ellipsoidal inclusions which are always more mafic than their host. The tonalite is especially rich in inclusions of this type (Fig. 3) and the composition of many of these xenoliths matches rock types found in the greenstone belts. These xenoliths appear to be blocks of the intrusion walls prised off by magmatic stoping which sank into the liquid magma because their density was slightly higher than that of the magma. Xenoliths are not abundant in the adamellitic granites and xenoliths are notably uncommon in the central parts of the intrusion. Those that do occur are mostly tonalitic or granodioritic in composition and, in contrast to the adamellite enclosing them, are often strongly schistose (Figs. 4 and 5). They are cognate xenoliths which were derived by stoping of previously solidified and deformed plutonic rocks. Dark amphibolitic and metasediment xenoliths locally occur in the central parts of the adamellite and it seems probable that the uppermost part of this intrusion locally broke through the previously intruded and consolidated tonalite roof to reach the outer envelope of greenstones. The xenoliths that are found in the western adamellite granite are all mafic rocks which can be matched with rocks found in the greenstone belt adjacent to the contacts.

The oblate ellipsoidal shapes of many of the xenoliths appear to result from deformation of the xenolith and its enclosing plutonic rock when both were in a plastic state. An analysis of the state of deformation described below suggests that the plastic flow occurred in the consolidated outer zones of the composite intrusion as new magmatic fluid was rising to fill and expand the central part of the mass.

Shear zones

Planar zones of anomalously high deformation occur throughout the batholith, but are especially common in the marginal tonalite. The width of the shear zones varies from a few centimetres to several metres, and pre-existing foliation or dyke structure are deflected sideways into the zone (Fig. 7). Although the layers are deflected they are not generally ruptured, and the strain variation across the shear zone shows no discontinuities. The schistosity within the shear zone is always stronger than that seen in the surrounding rock. If the walls of the shear zone are undeformed and without schistosity, then the schistosity in the shear zone makes an angle of about 45° to that of the zone. The deformations in these zones are interpreted as arising by simple shear. If the walls are schistose, however, the schistosity becomes stronger and makes a progressively smaller angle with the shear zone trace towards the centre of the zone (Fig. 8). The geometry of the structures in these zones is very like that described in areas of basement gneisses and massive

igneous rocks deformed by orogenic events (Ramsay & Graham 1970, Escher *et al.* 1975, Ramsay & Allison 1979).

The shear zones are vertical or steeply inclined. They occur in parallel sets with a similar sense of displacement or in crossing sets with the two directions making a conjugate arrangement of broadly synchronous aspect. One of the sets within a conjugate pattern always shows a right-hand subhorizontal sense of displacement and the other set shows a left-hand displacement. The overall displacement of conjugate sets is such as to cause an elongation of the rock mass along the direction of strike of the schistosity and a shortening in a direction approximately normal to the schistosity. The shear zones were probably produced during the later stages of the history of granite emplacement when displacements of the consolidated but ductile outer magmatic shell were predominantly subhorizontal and circumferencial.

Fractures

Regular fractures are seen to cut through the granite at many localities and they appear to be of several different generations. Those formed before the rocks had completely cooled are filled with hydrothermal material, usually quartz, chlorite, epidote and alkali feldspar. Extension fissures of this type are especially common in the outer zones of the adamellite and in the tonalites. They are generally steeply inclined and oriented at a high angle to the schistosity. They formed later than the main schistosity and cross-cut the latest intrusions of adamellitic pegmatites in the tonalite. At one locality (225625) xenoliths of tonalite inside the adamellite were cut by quartz–chlorite–epidote-filled fissures which stopped abruptly at the edge of the xenolith, and it would appear that these veins were formed before emplacement of the last stages of adamellite magma.

The latest fractures to form were steeply inclined extension and shear fractures which may or may not show differential movement. The joint spacing is very variable. The distance between adjacent joints is typically about 1 m, but in some of the central adamellite this may be as much as 50 m. No detailed work was done to establish the geometry of several joint sets or their age relationships.

Intrusive dykes and sheets

Dykes of fine-grained potassic granite, aplite and pegmatite are especially abundant in the tonalite and outermost zones of the adamellite. No general preferred orientation of the dykes could be seen but at some localities they appeared to be guided by foliation, schistosity and shear zones. From the disposition of structures in the dyke walls all the dykes are the result of dilation of the surrounding country rocks. Where dykes cut strongly schistose tonalite or adamellite a preferred alignment of the crystals within the dykes is seen, this being subparallel to the external schistosity. It appears that the dykes developed their schistosity during the time when the outer parts of the intrusion were being deformed.

The quartzo-feldspathic dykes which cut a large xenolith 7 km south of the centre of the adamellite (locality 194562) show remarkable deformation features. The thinnest dykes are folded into ptygmatic structures of very regular wavelengths and steeply inclined cross-cutting dykes show clear evidence of shortening in all directions within the subhorizontal outcrop surface (Snowden & Bickle 1976, plate 1b, Ramsay & Huber 1987, p. 68). Those dykes which are gently inclined show extraordinary dome and basin structure which confirm that the horizontal surface is one of strong shortening in all directions. The deformation has led to a strong decrease in area on this surface and it is accompanied by a marked steeply inclined linear stretching. The finite strain ellipsoid is therefore one of constrictional type. At this locality the deformed interface between granite and greenstone-belt material shows lobate–cuspate forms (Snowden & Bickle 1976, plate 1c). The cusp points are directed towards the granite, showing that the granite was more competent than the greenstone material (Ramsay 1967, p. 383).

BATHOLITH STRAIN AND EMPLACEMENT TECTONICS

Strain measurement

Many scientists investigating plutonic rocks have realized that the strain patterns produced by flow are likely to give valuable information concerning the kinematics of emplacement (Cloos 1936, Balk 1937, Ramsay 1975, Stephansson & Johnson 1976, Holder 1978, 1979, 1982, Pitcher 1979, Schwerdtner *et al.* 1983). The main problem of practical strain measurement is to find suitable objects of known initial geometry. It has been suggested that xenolith shapes might be used for such calculations (Balk 1937, Escorza 1978, Ramsay & Huber 1983). The Chindamora batholith offers particularly good material for this type of analysis.

The variation in intensity of the schistosity in the granite and the range of shapes of xenoliths suggested that there was a considerable variation in the amount of deformation through the batholith. At any one locality the xenoliths show a variety of shapes, but this variation appears to be consistent with what one expects from a homogeneous strain imposed on xenoliths with different initial shapes and different initial orientations (Ramsay 1967, pp. 202–216). In regions where the granites show little or no schistosity the xenoliths are variable in shape and their long axes appear to be poorly or randomly oriented. Where the granite shows a moderate schistosity the xenolith long axes show a greater preferred alignment with a scatter about the schistosity trace, and in regions where the schistosity is strongly developed the long axes are aligned almost perfectly parallel to the schistosity trace (Fig. 5). As the xenoliths become more

aligned the variation in ellipticity (ratio of lengths long axis and short axis) becomes greater.

Measurements of these geometric features can be used to compute the values of the finite strain and to remove the effects of the initial shape factor. There are several methods available for making this calculation. The R_f/ϕ' method (Ramsay 1967, p. 207, Dunnet 1969) assumes that the initial shapes are close to ellipsoids and that the strain is homogeneous from particle to matrix. This seems to be a reasonable assumption here. First, we have localities with undeformed xenoliths to study their initial form, and second the schistosity in deformed granites passes through the xenoliths without deflection, a feature implying strain homogeneity. The main problem with this technique is that it is very time consuming and a minimum of 50 deformed objects are considered to be required (Dunnet 1969). In the Chindamora batholith it is not common to find individual outcrops with so many measurable xenoliths and, furthermore, with the limited time that was available for the field investigation, it was considered more important to obtain many strain values of slightly inaccurate aspect rather than a few values of high accuracy. For this technique the geometric mean of individual xenolith ellipticities (r_1, r_2, r_3, . . ., r_n) was calculated. Dunnet (1969) and Lisle (1977) have shown that this mean gives a fairly close approximation to the ellipticity R of the finite strain ellipse on the surface:

$$R = \sqrt[n]{r_1\, r_2\, r_3 \ldots r_n}.$$

Values of R were calculated at 80 localities using as many individual xenoliths as possible, preferably at least 30. At each locality where the calculation could be made the strain ellipse shape, as seen on a horizontal outcrop surface, is illustrated in Fig. 9. In outcrops where vertical surfaces enabled three-dimensional calculations to be made it was found that the shape of the strain ellipse in a section normal to the schistosity was practically identical to that on the horizontal surface. The ellipsoids are of an almost perfect uniaxial oblate (pancake) type ($X = Y > Z$) with k-values (Flinn 1962, Ramsay & Huber 1983, p. 200) close to zero.

At five localities where greenstone xenoliths were found inside tonalite xenoliths within the adamellite intrusion core two strain ellipsoids could be computed, one representing the finite strain since the solidification of the tonalite, and the second indicating the strain since the consolidation of the adamellite. These computations are shown as double ellipses in Fig. 9.

Strain variation through the batholith

Figure 9 indicates the strain variation in the pluton. High strains are found in the tonalite and the lowest strains in the western marginal granite.

In order to see if there was any geometrically significant pattern of strain variation the value of $X/Y = Y/Z$ was plotted against distance from the central point C of

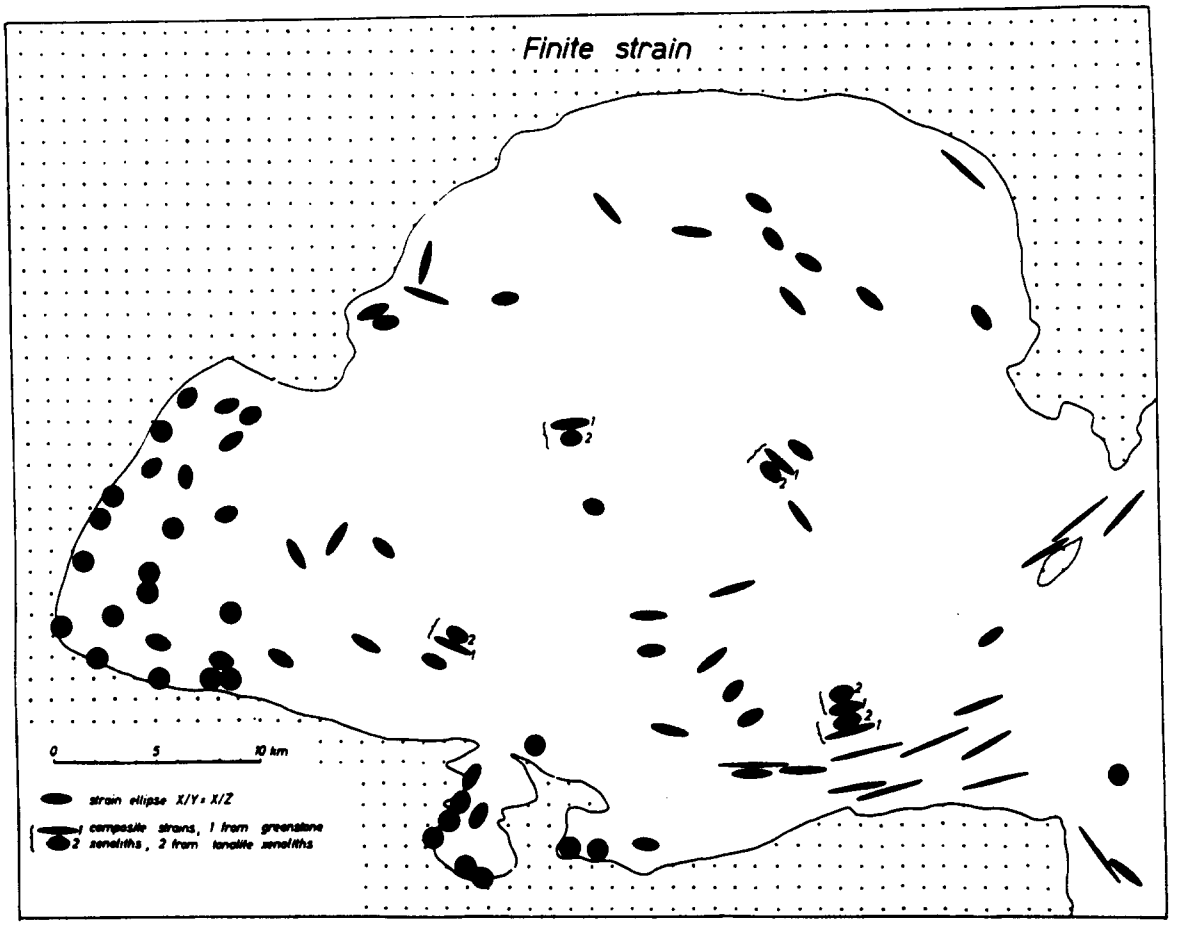

Fig. 9. Finite strains deduced from an analysis of xenolith shapes.

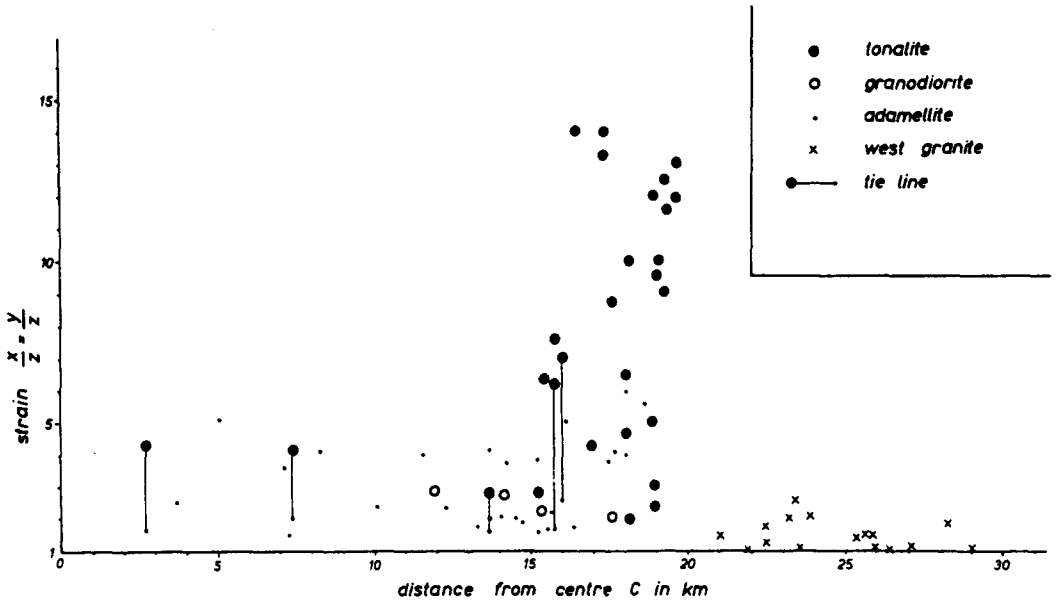

Fig. 10. Variation of strain state with distance from batholith centre (C in Fig. 2). The tie lines join strains determined from cognate xenoliths of tonalite in adamellite.

the batholith (Fig. 10 shows the data and Fig. 11 the general fields of strain). Where two strain ellipsoids could be computed (see above) these are joined with a tie line. The fields of strain in the tonalite, granodiorite and adamellite overlap, whereas the strain field in the western granite forms a distinct data set. The strain values fall into fairly distinct groups: the tonalite is characterized by moderate to very high strains, the adamellite generally low to moderate strains and the western granite shows consistently low strains. The strains derived from greenschist xenoliths within cognate tonalite xenoliths show a higher strain than that of the greenschist xenoliths in the main tonalite intrusion.

Although some workers attribute the strains within granitic plutons to the kinematic process of differential flow of a rising magma against the intrusion walls (Cloos 1936, Balk 1937, Bateman *et al.* 1963, 1983), the oblate uniaxial forms of the strain ellipsoids do not accord with such a displacement field. Upward flow of the magma against fixed walls would produce ellipsoids more in accord with simple shear ($X > Y > Z$ with $k = 1$ values), and with long axes plunging away from the intrusion centre at a lower inclination than the dip of the walls. The uniaxial symmetry, general parallelism of the XY ellipsoid plane with adjacent intrusion contacts, close association of S-planar fabric (schistosity) in conformity with the XY plane and general absence of linear fabrics seem to be more in accord with a 'balloon inflation' model (Pitcher & Berger 1972, Ramsay 1975, 1981, Holder 1978, 1979, Sylvester *et al.* 1978, Pitcher 1979). The model is that of stretching of the outer parts of the pluton together with the adjacent country rock envelope

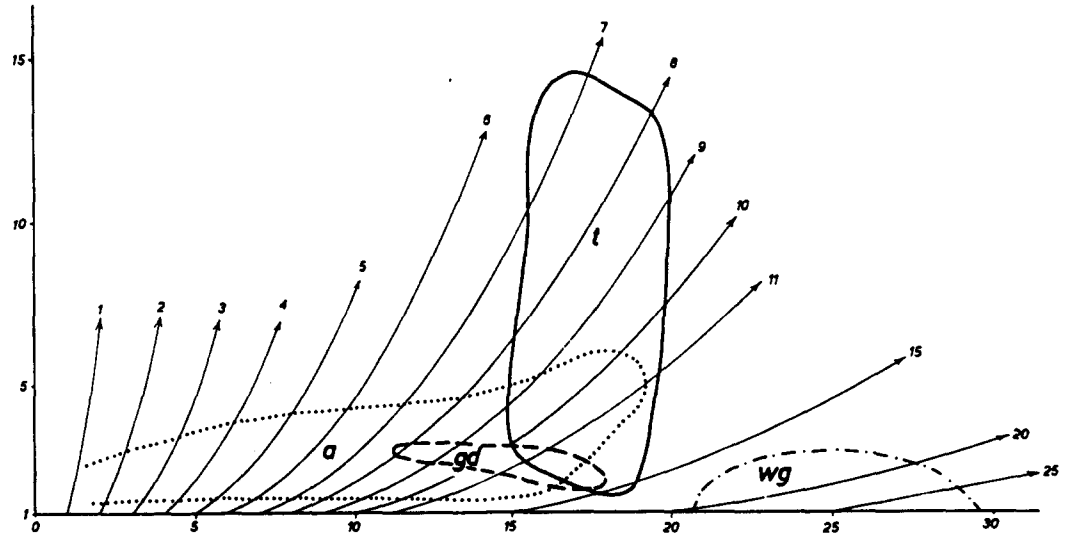

Fig. 11. Analysis of the main strain fields of Fig. 10 shown by tonalite t, adamellite a, granodiorite gd and western granite wg. The curved lines represent the deformation paths expected from xenoliths beginning their deformation at different distances (given by numbers 1, 2, . . ., 25 in km) from the centre C.

(Sylvester & Christie 1968) as a result of incoming of new magma into the pluton core much in the way that the skin of a rubber balloon is deformed as the balloon is inflated with air. The strain fields of the Chinadamora plutons are consistent with this model with progressive expansion of an outer (early intruded) tonalite, followed by granodiorite, followed by the central adamellite. This progressive balloon inflation was then followed by the last intrusion of the western granite along the tonalite–country rock interface and not in the balloon centre. This last intrusion phase did not lead to any geometric expansion of the previously formed diapir and the strains recorded inside the part of the intrusion are small and discordant to those of the adjacent igneous rocks (Fig. 11).

A MODEL TO EXPLAIN THE GEOMETRIC FEATURES OF THE CHINDAMORA BATHOLITH

Most geologists appear to accept that the granite plutons exposed at the surface today could have been developed and emplaced in several ways: by *in situ* high temperature metamorphism and melting ('granitization' of Read 1957) or by upward migration of relatively light density granitic magma or crystal–magma 'mush' through denser overburden rocks ('diapirism', Ramberg 1967, Berner *et al.* 1972, Stephansson 1974, Soula 1982) in a somewhat similar way to that by which salt diapirism occurs (Jackson & Talbot 1986). The overall geometric features of the Chindamora batholith accord best with the model of diapirism, although the plutonic rocks may well have initiated at depth by granitization and melting processes in the lower crust.

The consistency of cross-cutting relationships between plutonic rock types and the possibility of partitioning total strain into separate components associated with different magmatic types suggests that the diapiric activity was episodic, and that the magmatic balloon was filled by successive magma pulses. Data supporting episodic intrusion phenomena are relatively common in granitic terrains (Harry & Richey 1963, Bateman & Dodge 1970, Pitcher & Berger 1972, Stephansson 1974, Holder 1982). Although there is good evidence for periodicity of the Chindamora intrusion history it will be shown later that the overall kinematic pattern is suggestive of somewhat more continuous emplacement processes with special balancing between emplacement of fresh magma and consolidation of the earlier emplaced magmas.

The work of Balk (1937) suggested that the internal geometric features of plutons could always be subdivided into those which relate to primary magmatic flow and others which were produced after magma consolidation. Mineral alignments were attributed to orientation of solid crystal particles during magmatic flow. Berger & Pitcher (1970) queried these concepts and pointed out that many of the types of mineral fabrics seen in plutons can be matched in metamorphic terrains where no discrete magmatic phase appears to have existed (Debat *et al.* 1975). They suggested further that xenolith shapes owe their forms to the shape of the local deformation ellipsoid, implying that the host material did not have the properties of a true liquid, and that, because many examples are known where mineral alignment cross cuts the igneous banding, such fabrics were probably formed during a phase of deformation when the plutonic rock was in a plastic state. The observations made of fabric development and xenolith shapes in Chindamora support the conclusions of Berger & Pitcher (1970).

Where a magma retains fluid properties the overall stresses acting on an object (xenolith) carried along in the magma will be predominantly hydrostatic because the stress communication between the different parts of the fluid must be more or less equal. Any xenolith carried in the flow is therefore unlikely to be deformed because there are no high deviatoric stresses acting on its surface (Bateman *et al.* 1983). As soon as the magmatic fluid undergoes crystallization, however, the mechanical properties of the crystal mush become more complex. Where the fluid phase volumetrically predominates over the solid crystalline phases the overall magma will increase its viscosity with cooling, but will probably still retain its fundamental fluid properties. However, with further crystallization the solid components mechanically interact and the material reaction as a whole will become closer to that of a plastic solid. Once the crystal to crystal communication predominates, flow can take place only by crystal plasticity or chemical transfer at the highly stressed crystal interfaces. Differential stresses can now be transformed from point to point in the crystal aggregate and deformation of the interstitial magma and of the enclosing crystal particles can commence. It is suggested that there is some critical interfacial temperature controlled surface or zone in the magmatic mass where the magma properties change from those of a highly viscous fluid into those of a plastic (Van der Molen & Paterson 1979). In this zone the behaviour of the more or less homogeneous magmatic material will be governed by a change from predominantly hydrostatic stresses to strongly differential stresses. A coherent 'solid' xenolith in the magma passing through this transitional zone will therefore start to undergo a change in shape. The overall plastic shape changes in this rock mass will control the xenolith forms and crystal fabric.

Shaw (1965) and Murase & McBirney (1973) have noted a very rapid increase in magma viscosity with increasing crystallinity. Marsh (1984) has pointed out that lavas with more than 55% of phenocrysts are very rare implying that a magma–crystal 'mush' with a higher proportion of phenocrysts is too viscous to erupt at the surface. In plutons it seems certain that similar constraints on magma fluidity with degree of crystallization exist.

Various models have been proposed to account for the internal geometry of diapiric plutons. Mathematical and laboratory modelling techniques using various different types of model analogues have been described by Ramberg (1967, 1968, 1970), Berner *et al.* (1972),

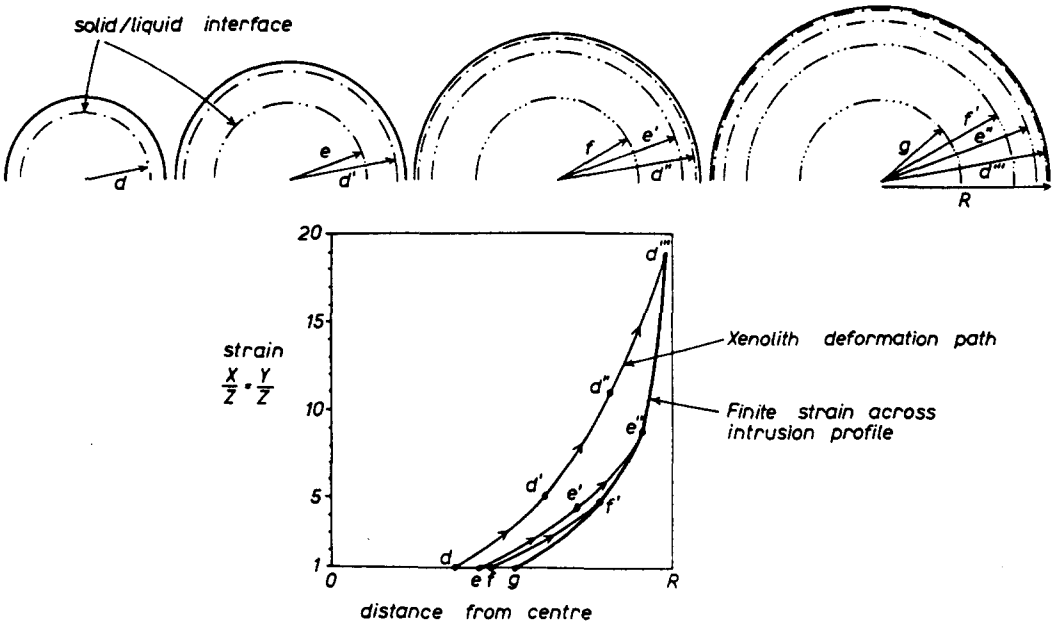

Fig. 12. Progressive inflation model (balloon model) used to calculate the relationships between strain state and distance from intrusion centre. A xenolith beginning its deformation history when it passes through the solid–liquid interface at distance d is moved radially outwards to distance d', d" and d'". The dash–dot lines show the positions of the solid–liquid interface (and deformed counterparts) as the pluton is inflated.

Fletcher (1972), Dixon (1975), Schwerdtner & Troëng (1978), Schwerdtner *et al.* (1978) and Morgan (1980). It has been shown that an initial swell may grow into a simple dome and how this dome may migrate upwards into 'tadpole' or 'reverse tear drop" form passing at late stages into a diapiric 'mushroom' perhaps completely disconnected from its original source layer. The possibility of developing the succession of forms depends upon the spacing of the initial instabilities, the thickness of the source and overburden layers, their densities and viscosities (Ramberg 1968, Berner *et al.* 1972, Schmeling 1987). Pitcher (1979) has pointed out that it is uncommon to find 'tadpole' and 'mushroom' forms in granitic plutons. Most plutons evolve only to the domal stage with a relatively low stage of diapirism. This is apparently the case with the Chindamora plutons and most of the other batholithic bodies of Zimbabwe. Probably the great size of these bodies relative to the thickness of the Archaean crust has inhibited the separation of bubble forms from the source material. Models of considerable complexity have been described to account for the forms of individual plutons: diapirism with tectonic compression from one side (Brun & Pons 1981), interference of adjacent pluton diapirs (Brun *et al.* 1981) and asymmetric diapirs resulting from complexities in the interfacial geometry of the surface between light source material and heavy overburden (Talbot 1977). Most of these seem inappropriate to the rather simple overall dome structure of the Chindamora batholith which appears to be best attributed to an evolution from a swelling blister into a half subspherical balloon.

A geometrically simple model will now be presented as a first approach to account for the observed strains in the Chindamora pluton. This model is based on the above discussion that deformation commences in the mass when an object, such as an included xenolith, passes through the fluid–plastic cooling front in the magma. The model is that of a simple spherically inflating balloon, fed from magma below, and which is undergoing cooling from the outside towards the inside. In this subspherical mass there is a spherical surface separating an inner fluid magmatic mass from an outer crystallized or partially crystallized shell which is undergoing a penetrative ductile stretch as a result of the overall inflation of the interior of the magma balloon. Any 'solid' or crystalline xenolith in the fluid part of the intrusion will remain undeformed or almost so. Where this xenolith passes through the fluid–plastic interface or front (Fig. 12, distance d from the pluton centre) it will start to be deformed. As the pluton becomes progressively infilled with new magmatic material the distance of the xenolithic strain marker from the central point of the magmatic balloon increases (d' to d" to d'") and the strain geometry is defined by the flattening stretch in the pluton skin. In a similar way more internally located xenoliths passing through the fluid–plastic front (at e, f and g) will also follow strictly determined strain–distance deformation paths (e, e', e", : f, f' : g) depending upon the distance at which they pass through the deformation front. All strain paths are fixed by the initial distance of the fluid–plastic interface from the intrusion centre. The distance travelled along any particular strain path depends upon the amount of subsequent stretching as a result of further filling of the magmatic balloon. The finite strain plan in the resulting pluton will mark the end points of successive individual deformation–distance paths. If the magmatic balloon geometry is subspherical then the strain in any xenolith can be used to define exactly the position in the intrusion where the xenolith passed through the fluid–plastic interface (Fig. 13).

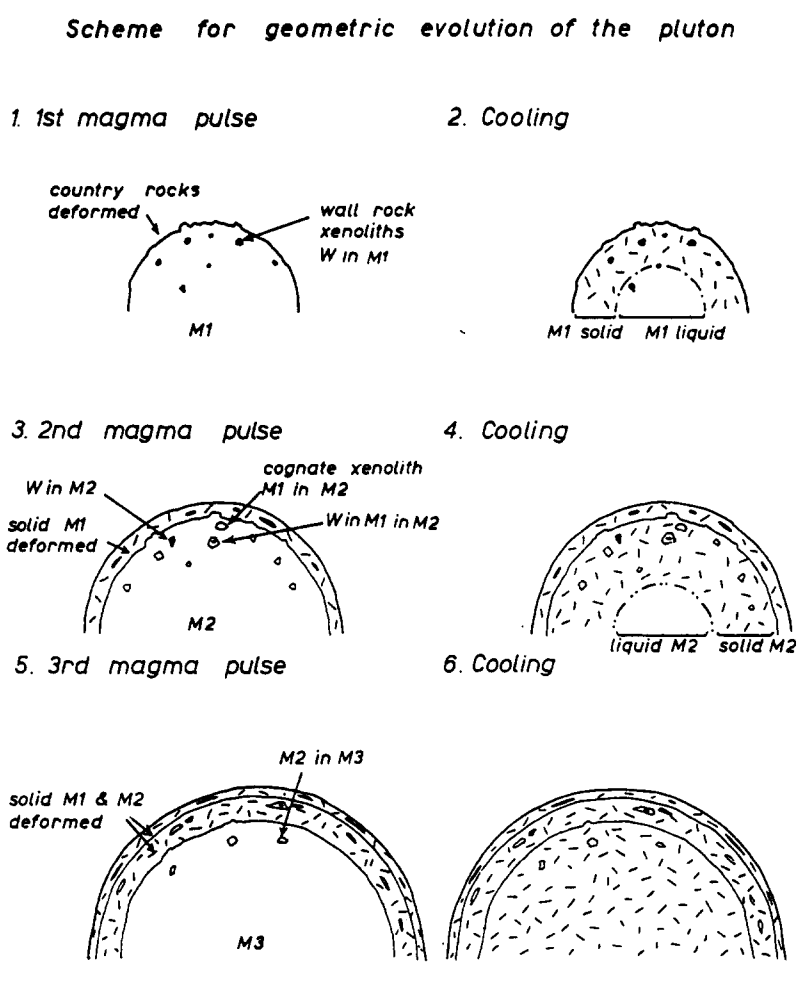

Fig. 13. Suggested scheme for the overall evolution of the Chindamora batholith. The magmas M1, M2 and M3 are tonalite, granodiorite and central adamellite respectively. Cooled and solidified (but plastic) rocks are ornamented with bars, liquid magma is unornamented.

The strain developed is a uniaxial oblate type. Assuming no volume change, the relation between the strain observed at any present distance d' from the intrusion centre and initial distance d (where the rock began its deformation history) is given by

$$R_{xy} = R_{xz} = (d'/d)^3,$$

where R_{xy} is the strain ratio on the XY principal plane, equivalent to the aspect ratio of the strain ellipse shown in Fig. 9. It follows from this relationship that it is possible to compute the distance d, the radius of the fluid–plastic interface for the volume of liquid magma existing at the time the xenolith passed through the cooling interface, knowing R_{xy} and d'.

The curved deformation–distance paths marked 1–25 in Fig. 11 were calculated from the equation above and can be used to interpret the strain fields of the different magma bodies as follows.

(1) The early formed tonalite was intruded as a body having a fluid–plastic interface of 6.5–15.0 km in diameter and was subsequently stretched to occupy its present position 15.0–20.0 km from the central point C.

(2) The later and rather localized granodiorite passed through a liquid–plastic interface located with a radius 8.0–15.0 km from the centre and was stretched to lie in its present position 11.0–18.0 km from the centre.

(3) The internal adamellite was intruded when the liquid–plastic interface was rapidly contracting relative to the rate of input of new magma from a radius of 14.0–0.0 km from the centre, and was stretched to lie in its present position 18.0–0.0 km from the centre.

(4) The western granite has a quite distinct deformation field from all the other magmatic components. It appears to have been initially intruded at a distance of 17.0–28.0 km from the central point of the whole pluton and was subsequently only very slightly stretched by the latest phase of plutonic activity.

Using these geometrical modelling techniques it is possible to construct the strain profile across plutons which have different intrusion increments vs cooling increments. The four models shown in Fig. 14 (a) show how plutons are inflated in 10 incremental volume stages ($\delta\Delta$) and how the volume (Δ) of the pluton progressively builds up during this magma input. The cooling rates are assumed to be constant through the period of intrusion. The different types of finite strain profile in the different intrusion sequences are extremely well demarcated (Fig. 14 b) and, although the geometrical analysis is based on what is undoubtedly an oversimplified description of reality, it is felt that the overall differences in the strain profiles predicted are so great that this technique might be of considerable interest to

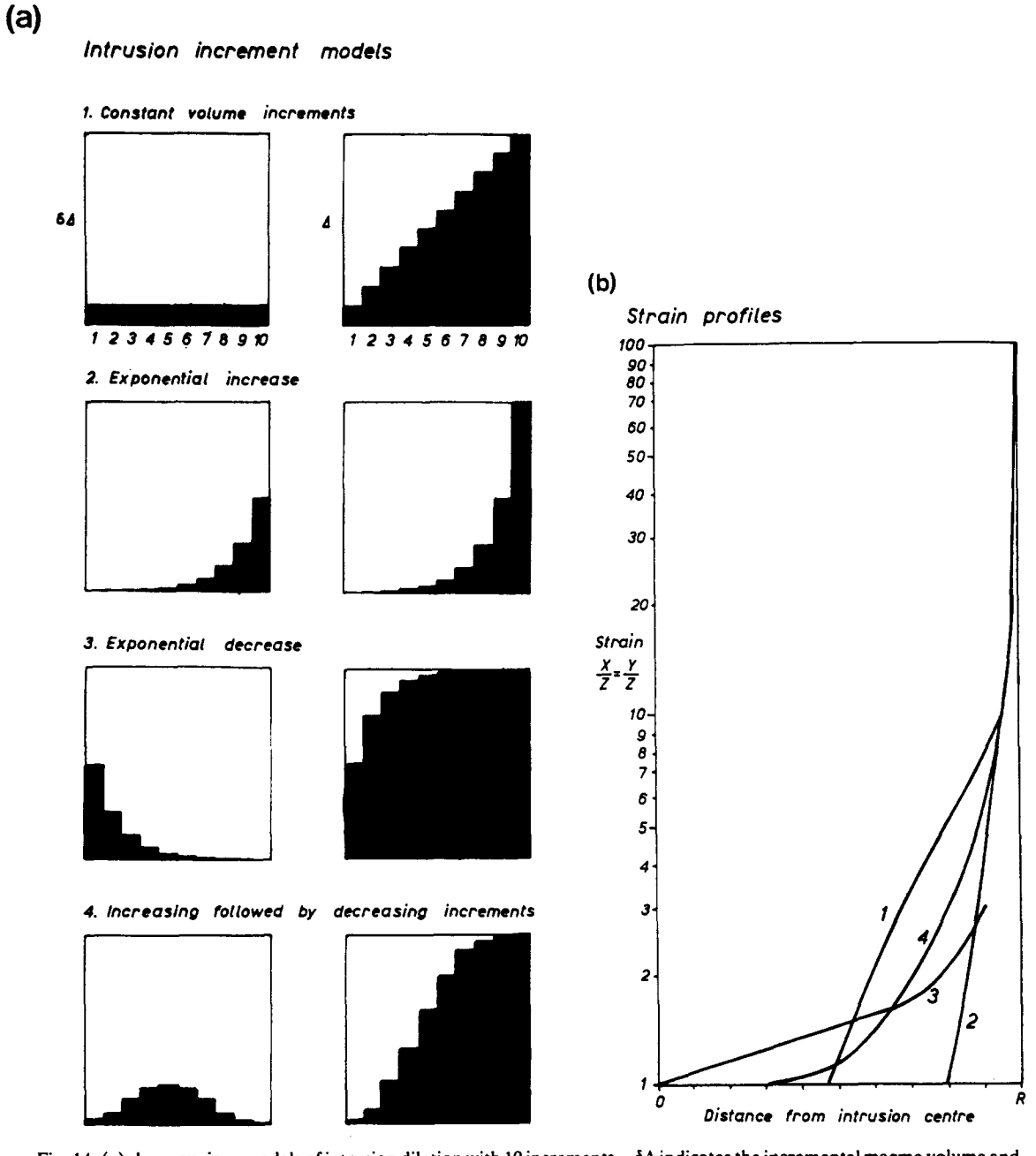

Fig. 14. (a) shows various models of intrusion dilation with 10 increments—$\delta\Delta$ indicates the incremental magma volume and Δ shows the proportion of the intrusion total volume relative to the final volume. (b) shows the types of finite strain profiles that would be anticipated from the four models set out in (a). These lines represent the end points of the individual deformation paths illustrated in Fig. 12.

determine the relative rates of infilling and solidification within a diapir.

Another way of presenting these data is shown in Figs. 15 and 16. This technique shows the position of the liquid–plastic solid interface (r) as the pluton evolves (with radius R). The data from the Chindamora pluton are presented in this form in Fig. 16. The early history of the intrusion is difficult to determine although the first tonalite body appears to have been inflated at a rate that was much higher than the cooling rate. There seems to have been a significant increase in the radius of the liquid core of the intrusion more or less coinciding with the arrival of granodiorite and adamellite magma. The inward migration of the fluid core at the later stages of the intrusion history in the main cooling phase is very clear, and this strong crystallization relative to volume of new magma of the central adamellite offers a good explanation for the lack of strain and mineral fabric in the intrusion centre. This figure does not incorporate the strain data from the marginal western granite, because the input of this magma was not centrally related to the diapir.

Shear zones

As a result of the incoming of the central part of the diapir the consolidated outer tonalitic skin was strongly stretched and the outermost parts of the adamellite were also circumferentially extended. This stretching appears to have led to the formation of single or conjugate sets of

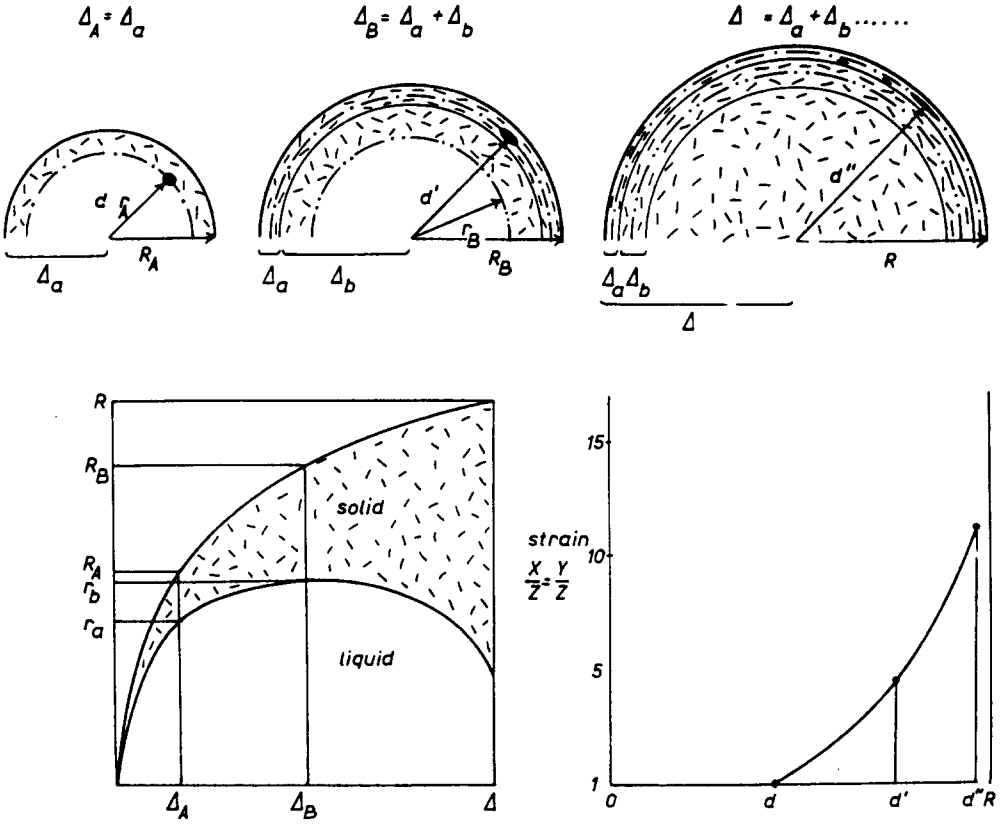

Fig. 15. Geometry of the balloon dilation model expressed as proportion of liquid and solid with progressive evolution of the pluton.

ductile shear zones in the intrusion envelope. The orientations of these shear zones and their right- or left-handed shear sense (looking down on a horizontal surface) are indicated in Fig. 17 (a). Where conjugate shear zones are found they appear to be broadly contemporaneous. The angles between such crossing zones have been bisected to give the directions of maximum bulk extensions. Having established the characteristic angles between conjugate shears it is possible to determine these principal strains from single parallel sets of shear zones. Figure 17 (b) shows the directions of maximum stretching at different localities in the pluton. These directions are, in general, parallel to the circumference of the pluton, and this geometry supports the idea of the initiation and development of shear zones as a result of inflation of the overall diapir by injection of new magma in the centre.

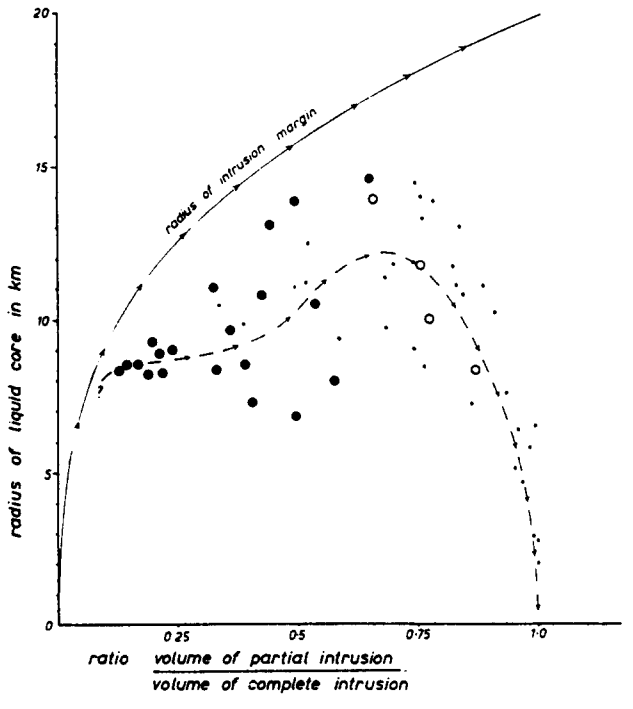

Fig. 16. Strain–distance data from the Chindamora batholith presented using the graphical technique of Fig. 15. Large dots tonalite, open circles granodiorite and small dots central adamellite. The dashed line shows the suggested changes in radius of the liquid core of the batholith as it is progressively inflated.

Special structural developments in the intrusion centre

In the central area of the adamellite, blocks of metasediment and greenstone of large dimensions (100 m diameter) are occasionally found. A point of special interest is that the strain in the inclusions, determined from the shapes of deformed conglomerates and folded aplitic and pegmatitic dykes, is quite high and of a constrictional type with steeply inclined maximum strain ($1 + e_1$) directions. In contrast, the strains in the immediately adjacent adamellite are typically small and show a flattening type of deformation. The interpretation of these rather unusual strains in the blocks is not completely clear. Snowden & Bickle (1976) have suggested that the overall dome-like nature of the Chindamora plutonic complex is the result of two separate regional deformations and not the result of diapiric rise.

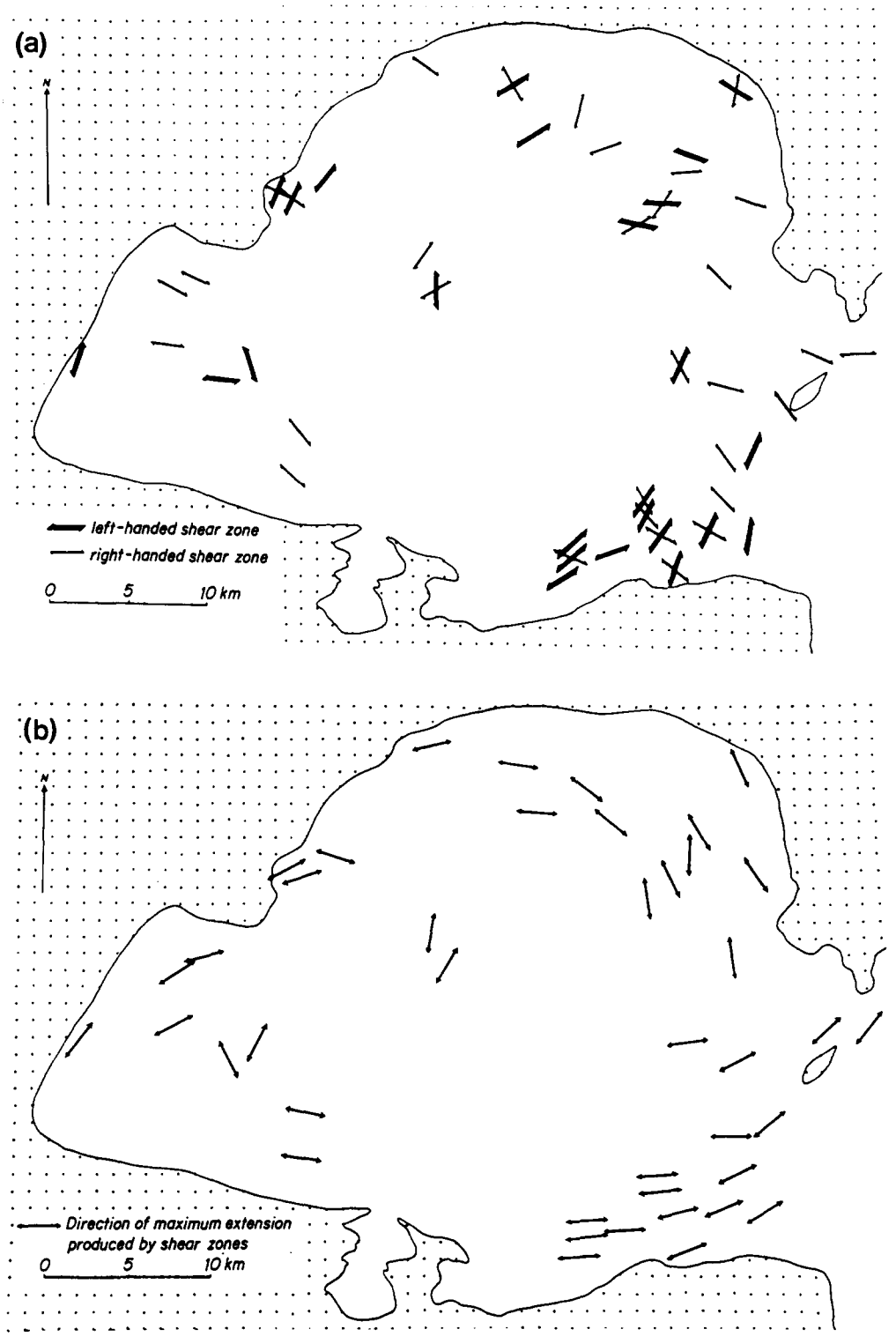

Fig. 17. (a). Orientations of right- and left-handed ductile shear zones in the Chindamora batholith. (b) Directions of maximum extension produced by the shear zones shown in (a).

They have therefore interpreted these complex structures and strains as resulting from the interference of successive folding phases. Although there are undoubted indications of more than one phase of deformational activity in the rocks of the greenstone belt surrounding the batholith I am not convinced that these phases are so ordered and of such equal intensity and style to have produced the oval forms of the plutonic masses we see at the surface today. Furthermore, the complex and rather irregular fold styles seen in the deformed dykes within the foreign blocks seem best interpreted as resulting from a single phase constrictional deformation and not from an interference of two phases of folding (Ramsay & Huber 1983, pp. 66–68). Another suggestion to account for these unusual structures is that the blocks might represent large xenoliths brought up from depth and containing strains characteristic of an intrusion 'stalk', although it has already

been pointed out that such a stalk is geometrically unlikely. In this reconnaissance study no clear solution to this problem was found.

CONCLUSIONS

The Chindamora batholith has a geometric form and internal strain field which can be attributed to successive diapiric rise of tonalite, granodiorite and adamellite about a common centre. The development of the diapir led to a 'balloon-like' inflation of the pluton and stretching of the outer consolidated but plastic igneous rocks and the formation of overall flattening strains. The western granitic mass shows features which are indicative of late emplacement on the side of the previously emplaced composite igneous pluton. Simple models based on spherical expansion of the mass can account for the observed strain pattern within the pluton. Although undoubtedly oversimplified, these models do suggest that field data and, in particular, the nature of the strain field might be used to evaluate the relative speeds of magma emplacement and magma solidification.

Acknowledgements—I would like to thank Chris Talbot and an anonymous reviewer for their comments and suggestions for improvement of the original manuscript.

REFERENCES

Anhaeusser, C. R., Mason, R., Viljoen, M. J. & Viljoen R. P. 1969. Reappraisal of some aspects of Precambrian shield geology. *Bull. geol. Soc. Am.* **80**, 2175–2200.

Balk, R. 1937. Structural behaviour of igneous rocks. *Mem. geol. Soc. Am.* **5**.

Bateman, P. C., Busacca, A. J. & Sawka, W. N. 1983. Cretaceous deformation in the western foothills of the Sierra Nevada, California. *Bull. geol. Soc. Am.* **94**, 30–42.

Bateman, P. C., Clark, L. C., Huber, N. K., Moore, J. G. & Rinehart, C. D. 1963. The Sierra Nevada batholith: a synthesis of recent work across the central part. *Prof. Pap. U.S. geol. Surv.* **414-D**.

Bateman, P. C. & Dodge, F. C. W. 1970. Variations of major chemical constituents across the Central Sierra Nevada Batholith. *Bull. geol. Soc. Am.* **81**, 409–420.

Berger, A. L. & Pitcher, W. S. 1970. Structures in granite rocks: a commentary and a critique on granite tectonics. *Proc. Geol. Ass. Lond.* **81**, 441–461.

Berner, H., Ramberg, H. & Stephansson, O. 1972. Diapirism in theory and experiment. *Tectonophysics* **15**, 197–218.

Brun, J.-P., Gapais, D. & Le Theoff, B. 1981. The mantled gneiss domes of Kuopio (Finland): interfering diapirs. *Tectonophysics* **74**, 283–304.

Brun, J.-P. & Pons, J. 1981. Strain patterns of pluton emplacement in a crust undergoing non-coaxial deformation. *J. Struct. Geol.* **3**, 219–229.

Cloos, E. 1936. Der Sierra Nevada Pluton in Californien. *Neues Jb. Geol. Palaent. Abh.* **76B**, 355–450.

Debat, P., Sirieys, P., Deramond, J. & Soula, J. C. 1975. Paleodéformations d'un massif orthogneissique. *Tectonophysics* **28**, 159–183.

Dixon, J. M. 1975. Finite strain and progressive deformation in models of diapiric structures. *Tectonophysics* **28**, 89–124.

Dunnet, D. 1969. A technique of finite strain analysis using elliptical particles. *Tectonophysics* **7**, 117–136.

Escher, A., Escher, J. C. & Waterson, J. 1975. The reorientation of the Kangâmiut dike swarm, West Greenland. *Can. J. Earth Sci.* **12**, 158–173.

Escorza, C. M. 1978. Estructura y deformación de los enclaves microgranulares negros (gabarros) del Alto de los Leones, Guadarrama. *Bol. R. Soc. Española Hist. Nat. (Geol.)* **76**, 57–87.

Fletcher, R. C. 1972. Application of a mathematical model to the emplacement of mantled gneiss domes. *Am. J. Sci.* **272**, 197–216.

Flinn, D. 1962. On folding during three dimensional progressive deformation. *J. geol. Soc. Lond.* **135**, 291–305.

Harry, W. T. & Richey, J. E. 1963. Magmatic pulses in the emplacement of plutons. *Liverpool Manchester geol. J.* **3**, 254–268.

Holder, M. T. 1978. Granite emplacement models. *J. geol. Soc. Lond.* **135**, 459–460.

Holder, M. T. 1979. An emplacement mechanism for post tectonic granites and its implications for their geochemical features. In: *Origin of Granite Batholiths—Geochemical Criteria* (edited by Atherton, M. P. & Tamey, J.). Shiva Pub. Co. Orpington, Kent, 116–128.

Holder, M. T. 1982. Mechanism of emplacement of granite plutons. Unpublished Ph.D thesis, University of Leeds.

Jackson, M. P. A. & Talbot, C. J. 1986. External shapes, strain rates and dynamics of salt structures. *Bull. geol. Soc. Am.* **97**, 305–323.

Lisle, R. J. 1977. Estimation of tectonic strain ratio from the mean shape of deformed elliptical markers. *Geol. Mijnb.* **56**, 140–144.

Marsh, B. D. 1984. Mechanics and energetics of magma formation and ascension. In: *Explosive Volcanism*. National Academy Press, Washington, 67–83.

McGregor, A. M. 1951. Some milestones in the Precambrian of Southern Rhodesia. *Geol. Soc. S. Africa Trans. & Proc.* **54**, 27–71.

Morgan, J. 1980. Deformation due to the distension of cylindrical igneous contacts: a kinematic model. *Tectonophysics* **66**, 167–178.

Murase, T. & McBirney, A. R. 1973. Properties of some common igneous rocks and their melts at high temperatures. *Bull. geol. Soc. Am.* **84**, 3563–3592.

Phaup, A. E. 1973. The granitic rocks of the Rhodesian Craton. *Spec. Publs geol. Soc. South Afr.* **3**, 59–67.

Pitcher, W. S. 1979. The nature, ascent and emplacement of granitic magmas. *J. geol. Soc. Lond.* **136**, 627–662.

Pitcher, W. S. & Berger, A. R. 1972. *The Geology of Donegal: A Study of Granite Emplacement and Unroofing*. Wiley Interscience, London.

Ramberg H. 1967. *Gravity, Deformation and the Earth's Crust*. Academic Press, London.

Ramberg, H. 1968. Fluid dynamics of layered systems in the field of gravity. *Phys. Earth & Planet. Interiors* **1**, 63–67.

Ramberg, H. 1970. Model studies in relation to intrusion of plutonic bodies. In: *Mechanism of Igneous Intrusion. Geol. J.* **2**, 261–286.

Ramsay, J. G. 1967. *Folding and Fracturing of Rocks*. McGraw Hill, New York

Ramsay, J. G. 1975. The structure of the Chindamora Batholith. *19th Ann. Rept. Res. Inst. African Geol. Univ. Leeds*, **81**.

Ramsay, J. G. 1981. Emplacement mechanics of the Chindamora Batholith, Zimbabwe. *J. Struct. Geol.* **3**, 93.

Ramsay, J. G. & Allison. I. 1979. Structural analysis of shear zones in an Alpinised Hercynian granite, Maggia Lappen, Pennine Zone, Central Alps. *Schweiz. Miner. Petrogr. Mitt.* **59**, 251–279.

Ramsay, J. G. & Graham, R. H. 1970. Strain variation in shear belts. *Can. J. Earth Sci.* **7**, 786–813.

Ramsay, J. G. & Huber, M. I. 1983. *The Techniques of Modern Structural Geology, Volume 1: Strain Analysis*. Academic Press, London.

Ramsay, J. G. & Huber, M. I. 1987. *The Techniques of Modern Structural Geology, Volume 2: Folds and Fractures*. Academic Press, London.

Read, H. H. 1957. *The Granite Controversy*. Murby & Co., London.

Schmeling, H. 1987. On the relation between initial conditions and late stages of Rayleigh-Taylor instabilities. *Tectonophysics* **133**, 65–80.

Schwerdtner, W. M. 1984. Foliation patterns in large gneiss bodies of the Archaean Wabigoon subprovince, southern Canadian Shield. *J. Geodynamics* **1**, 313–337.

Schwerdtner, W. M., Stott, G. M. & Sutcliffe, R. H. 1983. Strain patterns of crescentic granitoid plutons in the Archean greenstone terrain of Ontario. *J. Struct. Geol.* **5**, 49–430.

Schwerdtner, W. M., Sutcliffe, R. H. & Troëng, B. 1978. Patterns of total strain within the crestal region of immature diapirs. *Can. J. Earth Sci.* **15**, 1437–1447.

Schwerdtner, W. M. & Troëng, B. 1978. Strain distribution within arcuate diapiric ridges of silicone putty. *Tectonophysics* **50**, 13–28.

Shaw, H. R. 1965. Comments on viscosity, crystal settling and convection in granitic magmas. *Am. J. Sci.* **263**, 120–152.

Snowden, P. A. & Bickle, M. J. 1976. The Chindamora Batholith: diapiric intrusion or interference fold? *J. geol. Soc. Lond.* **132**, 131.

Snowden, P. A. & Snowden, D. V. 1979. Geology of an Archaean batholith, the Chindamora batholith, Rhodesia. *Trans. Geol. Soc. S. Africa* **82**, 7–22.

Snowden, P. A. & Snowden, D. V. 1981. Petrochemistry of the late

Archaean granites of the Chindamora batholith, Zimbabwe, *Precamb. Res.* **16**, 103–129.
Stephansson, O. 1972. Theoretical and experimental studies of diapiric structures on Oland. *Bull. geol. Inst. Univ. Uppsala* NS3, 163–200.
Stephansson, O. 1974. Polydiapirism of granite rocks in the Svecofenian of Central Sweden. *Precambrian Res.* **2**, 189–212.
Stephansson, O. & Johnson, K. 1976. Granite diapirism in the Rum Jungle area, Northern Australia. *Precambrian Res.* **3**, 159–187.
Soula, J. C. 1982. Characteristics and mode of emplacement of gneiss domes and plutonic domes in central-eastern Pyrenees. *J. Struct. Geol.* **4**, 313–342.
Sylvester, A. G. & Christie, J. M. 1968. The origin of crossed-girdle orientations of optic axes in deformed quartzites. *J. Geol.* **76**, 571–580.
Sylvester, A. G., Oertel, G., Nelson, C. A. & Christie, J. M. 1978. Papoose Flat pluton: a granitic blister in the Inyo Mountains, California. *Bull. geol. Soc. Am.* **89**, 1205–1219.
Talbot, C. J. 1968. Thermal convection in the Archaean crust? *Nature, Lond.* **220**, 552–556.
Talbot, C. J. 1977. Inclined and asymmetric upward-moving gravity structures. *Tectonophysics* **42**, 159–181.
Van der Molen, I. & Paterson, M. S. 1979. Experimental deformation of partially melted granite. *Contr. Miner. Petrol.* **70**, 299–318.
Viewing, K. A. & Harrison, N. M. 1973. A geological reconnaissance of the Chindamora batholith near Salisbury, Rhodesia. *Spec. Publs geol. Soc. South Afr.* **3**, 419–431.
Viljoen, M. A. & Viljoen, R. P. 1969. A reappraisal of the granite-greenstone terrains of shield areas on the Barberton model. *Spec. Publs geol. Soc. South Afr.* **2**, 245–274.